# Bayesian Mixed-Frequency Quantile Vector Autoregression: Eliciting tail risks of Monthly US GDP

Matteo Iacopini[*]    Aubrey Poon[†]    Luca Rossini[‡]    Dan Zhu[§]

September 7, 2022

## Abstract

Timely characterizations of risks in economic and financial systems play an essential role in both economic policy and private sector decisions. However, the informational content of low-frequency variables and the results from conditional mean models provide only limited evidence to investigate this problem. We propose a novel mixed-frequency quantile vector autoregression (MF-QVAR) model to address this issue. Inspired by the univariate Bayesian quantile regression literature, the multivariate asymmetric Laplace distribution is exploited under the Bayesian framework to form the likelihood. A data augmentation approach coupled with a precision sampler efficiently estimates the missing low-frequency variables at higher frequencies under the state-space representation.

The proposed methods allow us to nowcast conditional quantiles for multiple variables of interest and to derive quantile-related risk measures at high frequency, thus enabling timely policy interventions. The main application of the model is to nowcast conditional quantiles of the US GDP, which is strictly related to the quantification of Value-at-Risk and the Expected Shortfall.

**Keywords:** Bayesian inference; mixed-frequency; multivariate quantile regression; nowcasting; VAR.

---

[*]Queen Mary University of London, United Kingdom. `m.iacopini@qmul.ac.uk`

[†]Örebro University, Sweden. `aubrey.poon@oru.se`

[‡]University of Milan, Italy. `luca.rossini@unimi.it`

[§]Monash University, Australia. `dan.zhu@monash.edu`

1

# 1 Introduction

Most economic models' primary object of interest is the conditional mean of a given variable or index, as it summarizes the central response to explanatory variables. However, following the financial crises and economic shocks that characterized the last decade, policymakers and researchers have shifted their attention and interest beyond the conditional mean. In particular, the significant effects that exogenous shocks (such as the COVID-19 pandemic), wars (e.g., the Russian-Ukrainian war), and fluctuations of the business cycles have on the economy highlight the crucial need to investigate the tail and shoulders of the response variable's distribution.

Timely characterizations of risks to the economic outlook play a vital role in both economic policy and private sector decisions, where central bankers and analysts share a demand for timely forecasts of economic activity. To encapsulate and reflect the most recent events, forecasts of macroeconomic or financial variables should blend information collected from a wide array of sources and observed at different intervals or frequencies.

Moreover, research following the global financial crisis has provided substantial empirical evidence that the relationships among macroeconomic and financial time series are characterized by nonlinearities and asymmetries (Hubrich and Tetlow, 2015; Kilian and Vigfusson, 2017; Adrian et al., 2019). Thus, investigating the nonlinear effects related to cycles is crucial to policymakers for designing policies targeted at specific phases of the cycles. Researchers in macroeconomics usually base their analysis on linear regression methods, whereas only recently have nonlinear methods been applied to investigate economic policies and financial crises (e.g., Caggiano et al., 2022; Huber and Rossini, 2022). However, using conditional mean regression methods raises several concerns when modeling data with features such as skewness, fat tails, outliers, truncation, censoring and heteroscedasticity. This relates to the fact that the impact of covariates on the response may significantly vary across the range of the latter, thus highlighting the limitations of methods based on conditional mean only. The issue is ex-

acerbated by nonlinear relationships and non-Gaussian noises, typical features of many economic and financial variables.

In detecting economic and financial crises, appropriate risk measures are needed (Merlo et al., 2021), such as the Value at Risk (VaR) or the Expected Shortfall (ES). The VaR considers the maximum loss an operator can incur over a defined time horizon and for a given confidence level. At the same time, the ES coincides with the conditional expectation of exceedance beyond the VaR. In forecasting, Gneiting and Ranjan (2011) propose a threshold- and quantile-based decomposition of the continuously ranked probability score to assess density forecasting over the whole distribution and specific quantiles or regions of a variable of interest (e.g., the tails).

We introduce a novel mixed-frequency quantile vector autoregressive (MF-QVAR) model to address these issues. Unlike standard linear regression models, quantile regression (QR, see Koenker and Bassett, 1978) provides robust modeling of conditional quantiles. It allows the covariates to exert different impacts on each quantile level, thus enabling a comprehensive investigation of the entire conditional distribution. Following Petrella and Raponi (2019), we rely on the multivariate asymmetric Laplace (MAL) distribution to form the likelihood and conduct a simultaneous inference under the Bayesian framework on the marginal conditional quantiles of a multivariate response variable, taking into account the possible correlation among the marginals. Our framework permits the investigation of asymmetry in the downside and upside risks by considering different quantile levels, unlike standard models with symmetric second-moment dynamics. This quantile regression approach can be more effective, especially when skewness dynamics accompany the evolution of the distribution.

We build on the mixed frequency literature to exploit the information available at a higher frequency to nowcast quantiles of low-frequency variables of interest based on the state-space representation. The nowcasting and forecasting of multivariate quantiles would enable the policymakers to promptly detect early signals of distress and adopt corrective measures to counteract the early deterioration of the system. The proposed

approach automatically allows the forecaster to overcome the differences in data release dates that cause the available information set to differ over time within the quarter, so-called the "ragged-edge" problem.

To overcome the computational challenge in the mixed frequency VAR, we follow Chan et al. (2021), who designed a computationally efficient sampler for state-space models with missing observations, such as MF-VARs. They exploit the block-banded structure of the precision matrix of the conditional distribution of the missing observations to adapt the precision-based sampler of Chan and Jeliazkov (2009) to draw the missing low-frequency variables (see also Rue, 2001; Rue and Held, 2005). The importance of the precision sampler to modern econometric models is proven by its use in a variety of settings, including macro-econometric (Chan et al., 2013), models with missing observations (Hauber and Schumacher, 2021), and dynamic factor models (Kaufmann and Schumacher, 2019). An earlier method to make inference on unobserved variables in state space models is the simulation smoother (Durbin and Koopman, 2002, 2012). Moreover, we impose linear constraints when sampling the missing observations to ensure that missing high-frequency observations match the observed values of the low-frequency variables. This results in sampling from a linearly constrained Gaussian distribution, which is efficiently performed following the methods in Cong et al. (2017).

We apply our novel MF-QVAR model on a real-time nowcasting application for monthly US growth-at-risk. Specifically, we focus on the out-of-sample evaluation period between January 2016 and March 2022. During this evaluation period, we encounter ragged edges at the end of the sample as we respect the release calendar for all the monthly and quarterly variables included in our MF-QVAR model. In particular, we focus on generating the monthly nowcasts and forecasts under the three release timings of the US real GDP.

We found two key insights from our real-time nowcasting application. First, we show that there has been a downward shift in the monthly nowcasts of US growth-at-risk since the pandemic. For instance, the monthly nowcasts of US growth-at-risk were, on

average, about -3%, and this average dropped to about -5% during the pandemic period. Thus, this result implies that the monthly distribution of US real GDP has become more skewed to the left since the pandemic. Second, we compare our monthly nowcasts of US growth-at-risk to their corresponding quarterly nowcasts from the Adrian et al. (2019) quantile regression model. We found that, on average, the quarterly nowcasts underestimate US growth-at-risk relative to our monthly nowcasts. Furthermore, our monthly nowcasts of US growth-at-risk appear to align with the current post-pandemic economic situation in the US.

We also undertake a counterfactual analysis to investigate whether the Chicago Fed's National Financial Condition Index (NFCI) is important for nowcasting monthly US growth-at-risk. We compare our counterfactual monthly nowcasts to their corresponding actual monthly nowcasts. We found, on average, that a tightening of the NFCI does indeed have a negative impact on the monthly nowcast US growth-at-risk. Therefore, our results reinforce the findings of Adrian et al. (2019) and highlight the importance of including NFCI in a mixed frequency setting when modeling growth-at-risk.

The remainder of this article is organized as follows: Section 2 presents a novel mixed-frequency quantile VAR model under the acronym of MF-QVAR and the intertemporal constraints. In Section 3, the Bayesian approach for inference along with the posterior algorithm is described. Section 4 shows the results of a real data and a counterfactual analysis on US real GDP growth-at-risk. Finally, Section 5 draws the conclusions.

## 2 Mixed Frequency Quantile VAR

### 2.1 Notation

Let $\mathbb{S}^k = \{X \in \mathbb{R}^{k \times k} : X = X'\}$ denote the space of symmetric matrices of size $k \times k$ and $\mathbb{S}^k_{++} = \{X \in \mathbb{S}^k : \mathbf{a}'X\mathbf{a} > 0, \ \forall\, \mathbf{a} \in \mathbb{R}^k\}$ be the space of symmetric, positive definite matrices of size $k \times k$. For a matrix $A \in \mathbb{S}^k_{++}$, $A^{1/2}$ represents the Cholesky factor of

$A$. Let $\text{MAL}_n(\boldsymbol{\mu}, \boldsymbol{\delta}, \Sigma)$ indicate a multivariate asymmetric Laplace distribution with location $\boldsymbol{\mu} \in \mathbb{R}^n$, skewness parameter $\boldsymbol{\delta} \in \mathbb{R}^n$, and scale matrix $\Sigma \in \mathbb{S}_{++}^n$. Let $\mathbf{y}_t^o \in \mathbb{R}^{n_o}$ be a vector of variables observed at high frequency and let $\mathbf{y}_t^u \in \mathbb{R}^{n_u}$ be a vector of variables that are unobserved or only partially observed. Finally, let us denote with $I_n$ the identity matrix of size $n$, and use $\mathbf{1}_n$ and $\mathbf{0}_n$ to represent an $n$-dimensional vector with all entries equal to one and zero, respectively. The symbol $\otimes$ denotes the Kronecker product.

## 2.2 Model

We consider a $n$-dimensional VAR($p$) model with $p$ lags for $\mathbf{y}_t = (\mathbf{y}_t^{o'}, \mathbf{y}_y^{u'})'$, with $n = n_o + n_u$, that is

$$\mathbf{y}_t = \mathbf{b}_0 + \sum_{j=1}^{p} B_j \mathbf{y}_{t-j} + \boldsymbol{\epsilon}_t, \qquad \boldsymbol{\epsilon}_t \sim \text{MAL}_n(\mathbf{0}_n, D\boldsymbol{\theta}_{\tau,1}, D\boldsymbol{\theta}_{\tau,2}\Psi\boldsymbol{\theta}_{\tau,2}'D'), \qquad (1)$$

for $t = p + 1, \ldots, T$, where $\mathbf{b}_0$ is a $n$-dimensional vector of intercepts, $B_1, \ldots, B_p$ are $(n \times n)$ autoregressive coefficient matrices, $\Psi$ is a $(n \times n)$ correlation matrix, $D = \text{diag}\left(\Sigma_{11}^{1/2}, \ldots, \Sigma_{nn}^{1/2}\right)$, for $\Sigma_{ii}^{1/2} \in \mathbb{R}$, and

$$\boldsymbol{\theta}_{\tau,1} = \left(\frac{1 - 2\tau_1}{\tau_1(1 - \tau_1)}, \ldots, \frac{1 - 2\tau_n}{\tau_n(1 - \tau_n)}\right)', \qquad \boldsymbol{\theta}_{\tau,2} = \text{diag}\left(\sqrt{\frac{2}{\tau_1(1 - \tau_1)}}, \ldots, \sqrt{\frac{2}{\tau_n(1 - \tau_n)}}\right),$$

where $\boldsymbol{\tau} = (\tau_1, \ldots, \tau_n)$ is the quantile representation, such that $\tau_i \in (0, 1)$ for $i = 1, \ldots, n$.

The multivariate asymmetric Laplace distribution, $\text{MAL}_n(\boldsymbol{\mu}, D\boldsymbol{\theta}_{\tau,1}, D\boldsymbol{\theta}_{\tau,2}\Psi\boldsymbol{\theta}_{\tau,2}'D')$, has density function

$$f_Y(\mathbf{y}|\boldsymbol{\mu}, D\boldsymbol{\theta}_{\tau,1}, D\boldsymbol{\theta}_{\tau,2}\Psi\boldsymbol{\theta}_{\tau,2}'D') = \frac{2\exp\left\{(\mathbf{y} - \boldsymbol{\mu})'D^{-1}(\boldsymbol{\theta}_{\tau,2}\Psi\boldsymbol{\theta}_{\tau,2}')^{-1}\boldsymbol{\theta}_{\tau,1}\right\}}{(2\pi)^{n/2}|D\boldsymbol{\theta}_{\tau,2}\Psi\boldsymbol{\theta}_{\tau,2}'D|^{1/2}}\left(\frac{\tilde{m}}{2 + \tilde{d}}\right)^{\nu}K_\nu\left(\sqrt{(2 + \tilde{d})\tilde{m}}\right),$$

where $\tilde{m} = (\mathbf{y} - \boldsymbol{\mu})'(D\boldsymbol{\theta}_{\tau,2}\Psi\boldsymbol{\theta}_{\tau,2}'D')^{-1}(\mathbf{y} - \boldsymbol{\mu})$, $\tilde{d} = \boldsymbol{\theta}_{\tau,1}'\boldsymbol{\theta}_{\tau,2}\Psi\boldsymbol{\theta}_{\tau,2}'\boldsymbol{\theta}_{\tau,1}$ and $K_\nu(\cdot)$ denotes

the modified Bessel function of the third kind with index parameter $\nu = (2-n)/2$. The MAL distribution is closely related to multivariate quantile regression models, as stated in Proposition 1 from Petrella and Raponi (2019), which we report using our notation.

**Proposition 1** (Petrella and Raponi (2019)). *Let* $\mathbf{y} \sim \mathrm{MAL}_n(\boldsymbol{\mu}, D\boldsymbol{\theta}_{\tau,1}, D\boldsymbol{\theta}_{\tau,2}\Psi\boldsymbol{\theta}'_{\tau,2}D')$ *and let* $\boldsymbol{\tau} = (\tau_1, \ldots, \tau_n)'$ *be a fixed n-dimensional vector, such that* $\tau_i \in (0,1)$ *for* $i = 1, \ldots, n$. *Then* $\mathbb{P}(y_i \leq \mu_i) = \tau_i$ *if and only if*

$$\theta_{\tau,1,i} = \frac{1-2\tau_i}{\tau_i(1-\tau_i)}, \qquad \theta^2_{\tau,2,i} = \frac{2}{\tau_i(1-\tau_i)}.$$

*Moreover,* $y_i \sim \mathcal{AL}(\mu_i, \Sigma_{ii}^{1/2}, \tau_i)$ *follows a univariate asymmetric Laplace distribution (see Appendix A).*

Modern models for investigating macroeconomic and financial time series are inherently multivariate, which calls for developing suitable multivariate quantile regression models. Chavleishvili and Manganelli (2021) provide a structural quantile VAR (QVAR) model to capture nonlinear relationships among macroeconomic variables, and propose a quantile impulse response function to perform stress tests. Montes-Rojas (2019) develop a reduced form QVAR model to provide reliable forecasts and define a different quantile impulse response function to explore dynamic heterogeneity of the response variables to exogenous shocks. Recently, Adams et al. (2021) modified the approach of Adrian et al. (2019) and used quantile regressions to characterize upside and downside risks around the survey of professional forecasters' median consensus forecasts for each indicator.

The above-mentioned studies adopt a frequentist perspective. In contrast, Bernardi et al. (2015) developed a Bayesian inference for univariate quantile regression models to measure tail risk interdependence using Tobias and Brunnermeier (2016)'s Conditional VaR (CoVaR) indicator, defined as a quantile of a conditional distribution calculated at a given quantile of its conditioning distribution. Recently, Tian et al. (2021) exploited shrinkage priors to estimate Bayesian multivariate quantile regressions. Despite the

increasing interest by policymakers in understanding and forecasting the whole distribution of economic and financial indicators, the literature on quantile VAR models is scant. We aim to fill this gap by proposing a novel fast Bayesian approach to inference for quantile VAR models.

Following the literature on multivariate time series, we define the $n_\beta$-dimensional vector $\boldsymbol{\beta} = (\mathbf{b}_0', \text{vec}(B_1)', \ldots, \text{vec}(B_p)')'$, with $n_\beta = n(1 + np)$, and the $n \times n_\beta$-dimensional matrix $X_t = (\mathbf{1}_n, \mathbf{x}_{t,1}', \ldots, \mathbf{x}_{t,p}')$, with $\mathbf{x}_{t,j} = (\mathbf{y}_{t-j} \otimes I_n)$ for each $j = 1, \ldots, p$. Moreover, let us reparametrize the innovation scale by introducing the positive definite matrix $\Sigma = D\Psi D' \in \mathbb{S}_{++}^n$, and relabelling with $D = D(\Sigma) = \text{diag}\left(\Sigma_{11}^{1/2}, \ldots, \Sigma_{nn}^{1/2}\right)$. Owing to the properties of the multivariate asymmetric Laplace distribution, eq. (1) admits a representation as a location-scale mixture of Gaussian distributions (Petrella and Raponi, 2019; Kotz et al., 2001), as follows:

$$\mathbf{y}_t = \mathbf{b}_0 + \sum_{j=1}^{p} B_j \mathbf{y}_{t-j} + D\boldsymbol{\theta}_{\tau,1} w_t + \sqrt{w_t} D\boldsymbol{\theta}_{\tau,2}\Psi^{1/2}\tilde{\mathbf{z}}_t, \qquad \tilde{\mathbf{z}}_t \sim \mathcal{N}_n(\mathbf{0}_n, I_n), \qquad (2)$$

$$= X_t\boldsymbol{\beta} + D(\Sigma)\boldsymbol{\theta}_{\tau,1} w_t + \mathbf{z}_t, \qquad \mathbf{z}_t \sim \mathcal{N}_n(\mathbf{0}_n, w_t\boldsymbol{\theta}_{\tau,2}\Sigma\boldsymbol{\theta}_{\tau,2}), \qquad (3)$$

where $w_t$ is an auxiliary variable satisfying[1] $w_t \overset{i.i.d.}{\sim} \mathcal{E}xp(1)$, and define $\mathbf{w} = (w_{p+1}, \ldots, w_T)'$ the vector of latent variables.

## 2.3 Mixed Frequency and Inter-Temporal Constraints

Mixed frequency VAR (MF-VAR) models in macroeconomics and forecasting have become increasingly popular for producing high-frequency nowcasts of low-frequency variables. Specifically, MF-VARs are often used to joint model quarterly macroeconomic variables (low-frequency), such as gross domestic product (GDP), and monthly financial variables (high-frequency), such as surveys, to produce monthly nowcasts of GDP (e.g., see Schorfheide and Song, 2015).

---

[1]We use the rate parametrization, such that if $x \sim \mathcal{E}xp(1)$, then $kx \sim \mathcal{E}xp(1/k)$, for $k > 0$.

We contribute to this literature by introducing mixed-frequency components in quantile VAR models that allow us to nowcast the conditional mean and the distribution of the low-frequency variables of interest. This is of paramount importance to timely understand the status of the economic system by explaining and nowcasting fundamental indicators, such as GDP and systemic risk indices. Moreover, it allows the researchers to consider any ragged-edge issues arising from the data release calendar.

A stacked or a state-space approach can be used to handle the mixed-frequency variables. The first class includes the MIDAS models, initially proposed by Ghysels et al. (2005, 2006) and Ghysels (2016), which consist of a linear model for the lowest observed frequency that includes the high-frequency covariates using particular functional forms for the coefficients. This framework has recently been extended to account for multiple regimes, dynamic panels, and high-dimensional settings (e.g., see Casarin et al., 2018; Khalaf et al., 2021; Mogliani and Simoni, 2021). Conversely, the state-space approach proposed by Schorfheide and Song (2015) treats the high-frequency observations of the low-frequency variables as missing values and estimates them via Kalman filtering and smoothing algorithms. This method has been applied to investigate consumption growth and long-run risks (Schorfheide et al., 2018), the COVID-19 outbreak (Huber et al., 2020), the output gap (Cimadomo et al., 2021), regional output growth (Koop et al., 2020), and high-dimensional macroeconomic systems (Berger et al., 2020).

In particular, we adopt the state-space approach and model all variables at the highest observed frequency to obtain the interpolated estimates of the low-frequency variables at a higher frequency. The main drawback of this approach is the significant computational burden mainly due to the estimation of high-dimensional latent state vectors (i.e., missing observations of the low-frequency variables) via filtering and smoothing techniques. This cost becomes prohibitive as the dimension of the VAR gets large, thus representing a major obstacle to using state-space methods on datasets with medium-high dimensions.

To investigate the joint distribution of the unobserved variables, conditional on the

observations, let us denote with $\mathbf{Y} = (\mathbf{y}'_{p+1}, \ldots, \mathbf{y}'_T)'$ and $\boldsymbol{\zeta} = (\mathbf{z}'_{p+1}, \ldots, \mathbf{z}'_T)'$ the $(T-p)n$-dimensional vectors obtained by stacking all observations and all innovations over time, respectively. It is now possible to rewrite eq. (2) in matrix form as:

$$\mathbf{BY} = \mathbf{b} + \boldsymbol{\zeta}, \qquad \boldsymbol{\zeta} \sim \mathcal{N}(\mathbf{0}_{(T-p)n}, \boldsymbol{\Sigma}), \tag{4}$$

where

$$\mathbf{b} = (\mathbf{1}_{T-p} \otimes \mathbf{b}_0) + \mathbf{w} \otimes \left( \frac{(1-2\tau_1)\Sigma_{11}^{1/2}}{\tau_1(1-\tau_1)}, \ldots, \frac{(1-2\tau_n)\Sigma_{nn}^{1/2}}{\tau_n(1-\tau_n)} \right)', \qquad \boldsymbol{\Sigma} = \mathrm{diag}(\mathbf{w}) \otimes \boldsymbol{\theta}_{\tau,2} \Sigma \boldsymbol{\theta}_{\tau,2},$$

and

$$\mathbf{B} = \begin{bmatrix} -B_1 & -B_2 & \ldots & -B_p & I_n & \mathbf{0}_n & \ldots & \mathbf{0}_n & \mathbf{0}_n & \mathbf{0}_n \\ \mathbf{0}_n & -B_1 & \ldots & -B_{p-1} & B_p & I_n & \ldots & \mathbf{0}_n & \mathbf{0}_n & \mathbf{0}_n \\ \ldots & \ldots & \ldots & \ldots & \ldots & \ldots & \ldots & \ldots & \ldots & \ldots \\ \mathbf{0}_n & \mathbf{0}_n & \ldots & \mathbf{0}_n & \mathbf{0}_n & \mathbf{0}_n & \ldots & -B_p & I_n & \mathbf{0}_n \\ \mathbf{0}_n & \mathbf{0}_n & \ldots & \mathbf{0}_n & \mathbf{0}_n & \mathbf{0}_n & \mathbf{0}_n & -B_{p-1} & -B_p & I_n \end{bmatrix}$$

as a banded matrix of dimensionality $(Tn \times (T-p)n)$. Notice that $\mathbf{b}$, $\boldsymbol{\Sigma}$, and $\mathbf{B}$ depend on the model parameters; we drop the notation for exposition purposes.

As stated in Schorfheide and Song (2015), we formulate the mixed frequency VAR in a state-space structure. To this aim, let us first denote with $\mathbf{y}^o = (\mathbf{y}_1^{o'}, \ldots, \mathbf{y}_T^{o'})'$ and $\mathbf{y}^u = (\mathbf{y}_1^{u'}, \ldots, \mathbf{y}_T^{u'})'$ the $Tn_o$- and $Tn_u$-dimensional stacked vectors of observed and unobserved response variables. This allows to represent the vector $\mathbf{y}$ as a linear combination of $\mathbf{y}^o$ and $\mathbf{y}^u$, as follows:

$$\mathbf{y} = M_u \mathbf{y}^u + M_o \mathbf{y}^o, \tag{5}$$

where $M_o$ and $M_u$ are $(Tn \times Tn_o)$ and $(Tn \times Tn_u)$ selection matrices with full column rank. Then, by substituting eq. (5) into eq. (4) along the lines of Chan et al. (2021), one

obtains the joint distribution of the missing observations, conditional on the observed data and model parameters as the Gaussian distribution:

$$\mathbf{y}^u | \mathbf{y}^o, \boldsymbol{\beta}, \Sigma, \mathbf{w} \sim \mathcal{N}(\boldsymbol{\mu}_y, K_y^{-1}), \tag{6}$$

where $K_y = M_u' \mathbf{B}' \boldsymbol{\Sigma}^{-1} \mathbf{B} M_u$ and $\boldsymbol{\mu}_y = K_y^{-1} \left( M_u' \mathbf{B}' \boldsymbol{\Sigma}^{-1} \left( \mathbf{b} - \mathbf{B} M_o \mathbf{y}^o \right) \right)$.

In practice, the unobserved data points in $\mathbf{y}^u$ are constrained to match the value of the low-frequency variables at those points in time when the latter are observed. One of the most commonly used restrictions for log-differenced variables is the log-linear approximation of Mariano and Murasawa (2003, 2010). This approach assumes that the observed quarterly value of the $i$-th variable at month $t$, denoted by $\tilde{y}_{i,t}^u$, is obtained as a linear combination of the missing monthly values at the current and previous four months, denoted by $y_{i,t}^u, \ldots, y_{i,t-4}^u$, as follows:

$$\tilde{y}_{i,t}^u = \frac{1}{3} y_{i,t}^u + \frac{2}{3} y_{i,t-1}^u + y_{i,t-2}^u + \frac{2}{3} y_{i,t-3}^u + \frac{1}{3} y_{i,t-4}^u. \tag{7}$$

This is a log-linear approximation to an arithmetic average of the quarterly variable, where note that $\tilde{y}_{i,t}^u$ is only observed for every third month. Stacking the inter-temporal constraints over time, one gets

$$\tilde{\mathbf{y}}^u = M_a \mathbf{y}^u, \tag{8}$$

where $M_a$ is a $(k \times T n_u)$ matrix containing the $k$ linear restrictions, and $\tilde{\mathbf{y}}^u$ is a vector containing the observed values of the low-frequency variables. To account for the inter-temporal constraints when sampling the unobserved variables, $\mathbf{y}^u$, it is sufficient to draw from the Gaussian distribution in eq. (6) subject to the restrictions in eq. (8). This is efficiently done following the methods described in Algorithm 2 of Cong et al. (2017), which postulates first to draw a vector from the unconstrained distribution,

$\mathbf{u} \sim \mathcal{N}(\boldsymbol{\mu}_y, K_y^{-1})$, then compute

$$\mathbf{y}^u = \mathbf{u} + K_y^{-1} M_a' (M_a K_y^{-1} M_a')^{-1} (\tilde{\mathbf{y}}^u - M_a \mathbf{u}). \tag{9}$$

From a computational perspective, we follow the efficient implementation in Algorithm 1 of Chan et al. (2021).

# 3 Bayesian inference

In this section, we provide the details of the estimation of our proposed MF-QVAR model. Initially, we exploit the location-scale mixture representation of the multivariate asymmetric Laplace in eq. (1) and introduce a set of auxiliary variables $w_t \overset{i.i.d.}{\sim} \mathcal{E}xp(1)$, thus the complete-data likelihood is given by:

$$
\begin{aligned}
L((\mathbf{y}_1^o, \mathbf{y}_1^u), \ldots, (\mathbf{y}_T^o, \mathbf{y}_T^u), \mathbf{w}|\boldsymbol{\beta}, \Sigma) &= \prod_{t=p+1}^{T} P(\mathbf{y}_t|\boldsymbol{\beta}, \Sigma, w_t) P(w_t|\boldsymbol{\beta}, \Sigma) \\
&= \prod_{t=p+1}^{T} \exp \left\{ -\frac{1}{2} \Big[ \big(\mathbf{y}_t - X_t\boldsymbol{\beta} - D(\Sigma)\boldsymbol{\theta}_{\tau,1}\big)' \big(w_t \boldsymbol{\theta}_{\tau,2} \Sigma \boldsymbol{\theta}_{\tau,2}\big)^{-1} \big(\mathbf{y}_t - X_t\boldsymbol{\beta} - D(\Sigma)\boldsymbol{\theta}_{\tau,1}\big) \Big] \right\} \\
&\quad \times (2\pi)^{-\frac{n}{2}} |w_t \boldsymbol{\theta}_{\tau,2} \Sigma \boldsymbol{\theta}_{\tau,2}|^{-\frac{n}{2}} \exp\{-w_t\}.
\end{aligned} \tag{10}
$$

Before describing the posterior distributions along with the algorithm used, we define the prior specifications for our parameters. Starting with the coefficient vector $\boldsymbol{\beta} = (\mathbf{b}_0', \text{vec}(B_1, \ldots, B_p)')'$, we assume a conjugate multivariate Gaussian prior distribution

$$\boldsymbol{\beta} \sim \mathcal{N}_{n_\beta}(\underline{\boldsymbol{\mu}}_\beta, \underline{\Omega}_\beta).$$

For this vector of coefficients, one may consider using shrinkage priors such as the global-local shrinkage prior (Polson and Scott, 2010; Bhadra et al., 2016), and the Minnesota prior (Kadiyala and Karlsson, 1997). In this article, we focus on a simple case by setting the prior mean of the coefficient associated with each equation at the frequentist

univariate regression estimate, $\underline{\boldsymbol{\mu}}_\beta = \widehat{\boldsymbol{\beta}}$, and a prior variance $\underline{\Omega}_\beta = 100 \cdot I_{n_\beta}$, which results in a relatively flat prior distribution. We leave for further research the use of more complex shrinkage priors.

The other parameter of interest is the scale matrix, $\Sigma \in \mathbb{S}_{++}^n$, and in this scenario, we assume an inverse Wishart prior distribution

$$\Sigma \sim \mathcal{IW}_n(\underline{\nu}_0, \ \underline{\Phi}_0),$$

where $\underline{\nu}_0 > n - 1$ is the degrees of freedom parameter and $\underline{\Phi}_0 \in \mathbb{S}_{++}^n$ is a scale matrix, such that if $\underline{\nu}_0 > n + 1$ then $\mathbb{E}[\Sigma] = \underline{\Phi}_0/(\underline{\nu}_0 - n - 1)$. This is equivalent to assuming the Wishart prior distribution for $\Sigma^{-1} \sim \mathcal{W}_n(\underline{\nu}_0, \ \underline{\Phi}_0^{-1})$, where $\mathbb{E}[\Sigma^{-1}] = \underline{\Phi}_0^{-1}\underline{\nu}_0$.

Based on these prior specifications and the likelihood function in eq. (10), we can provide the full conditional distributions for each parameter and latent variable of the model. We remark that our parametrization differs from Tian et al. (2016), as we work with the positive definite matrix $\Sigma$, instead of the correlation matrix $\Psi$ and the diagonal matrix $D$ separately. Moreover, we work with multivariate Bayesian analysis of quantile regression models, while Yu and Moyeed (2001) proposed a Bayesian approach for the univariate framework.

As the joint posterior distribution is not tractable, we rely on data augmentation to obtain closed-form full conditional distributions and to design an efficient Markov chain Monte Carlo (MCMC) algorithm for approximating the posterior distribution. Specifically, we design an efficient Gibbs sampler based on the precision sampler of Chan and Jeliazkov (2009) and Chan et al. (2021), which cycles over the following steps:

1. draw $\mathbf{y}^u$ given $\mathbf{y}^o, \boldsymbol{\beta}, \mathbf{w}$ and $\Sigma$ from eq. (6) subject to the restrictions in eq. (8) using Algorithm 1 of Chan et al. (2021);

2. draw $\boldsymbol{\beta}$ given $\mathbf{y}^o, \mathbf{y}^u, \mathbf{w}$ and $\Sigma$ from the Gaussian distribution $\mathcal{N}_{n_\beta}(\overline{\boldsymbol{\mu}}_b, \overline{\Omega}_b)$, with

$\tilde{\mathbf{e}}_t = \mathbf{y}_t - D\boldsymbol{\theta}_{\tau,1}w_t$ and parameters

$$\overline{\Omega}_b = \left(\underline{\Omega}_b^{-1} + \sum_{t=p+1}^{T} X_t'(w_t\boldsymbol{\theta}_{\tau,2}\Sigma\boldsymbol{\theta}_{\tau,2})^{-1}X_t\right)^{-1}, \quad \overline{\boldsymbol{\mu}}_b = \overline{\Omega}_b^{-1}\left(\underline{\Omega}_b^{-1}\underline{\boldsymbol{\mu}}_b + \sum_{t=p+1}^{T} \tilde{\mathbf{e}}_t'(w_t\boldsymbol{\theta}_{\tau,2}\Sigma\boldsymbol{\theta}_{\tau,2})^{-1}X_t\right).$$

3. draw the auxiliary variables $w_t$, for each $t = p+1, \ldots, T$, given $\mathbf{y}^o, \mathbf{y}^u, \boldsymbol{\beta}$ and $\Sigma$ from the Generalized inverse Gaussian distribution $\mathrm{GiG}(\overline{p}_w, \overline{a}_w, \overline{b}_{w,t})$, with $\mathbf{u}_t = \mathbf{y}_t - X_t\boldsymbol{\beta}$, and

$$\overline{p}_w = 1 - \frac{n}{2}, \qquad \overline{a}_w = 2 + \boldsymbol{\theta}_{\tau,1}'D(\boldsymbol{\theta}_{\tau,2}\Sigma\boldsymbol{\theta}_{\tau,2})^{-1}D\boldsymbol{\theta}_{\tau,1}, \qquad \overline{b}_{w,t} = \mathbf{u}_t'(\boldsymbol{\theta}_{\tau,2}\Sigma\boldsymbol{\theta}_{\tau,2})^{-1}\mathbf{u}_t.$$

4. draw $\Sigma$ given $\mathbf{y}^o, \mathbf{y}^u, \boldsymbol{\beta}$ and $\mathbf{w}$ via the slice sampling algorithm of Neal (2003). Defining $\mathbf{e}_t(\Sigma) = \mathbf{y}_t - X_t\boldsymbol{\beta} - D(\Sigma)\boldsymbol{\theta}_{\tau,1}w_t$, the target density function is proportional to:

$$\propto |\Sigma|^{-\frac{\nu_0+n+1}{2}} \exp\left\{-\frac{1}{2}\operatorname{tr}\left(\underline{\Phi}_0\Sigma^{-1}\right)\right\} |\Sigma|^{-\frac{T}{2}} \exp\left\{-\frac{1}{2}\sum_{t=1}^{T} \mathbf{e}_t'(\Sigma)\left(w_t^{-1}\boldsymbol{\theta}_{\tau,2}^{-1}\Sigma^{-1}\boldsymbol{\theta}_{\tau,2}^{-1}\right)\mathbf{e}_t(\Sigma)\right\}.$$

The Supplementary Material provides a detailed description of the MCMC algorithm along with the derivation of the full conditional distributions.

# 4   Nowcasting Monthly US GDP growth-at-risk

We illustrate the utility of our proposed MF-QVAR model by undertaking a real-time nowcasting application for the growth-at-risk of US real GDP. To the best of our knowledge, this is the first study in the literature that explicitly nowcasts a monthly growth-at-risk estimate for US real GDP, whereas all the previous studies only modeled it at a quarterly frequency. A key advantage of our MF-QVAR model is that it *naturally* allows the forecaster to consider any ragged-edge issues arising from the data release calendar.

We estimate an MF-QVAR model consisting of the quarterly US real GDP and eight

monthly variables. Seven of the monthly variables included in our model are broadly similar to the monthly variables chosen in Schorfheide and Song (2015) standard MF-VAR model, whereas the last one is the NFCI. This choice is motivated by the recent study of Adrian et al. (2019), which showed that a tightening of the NFCI could lead to a large increase in the growth-at-risk for US real GDP. Table 1 reports the details of each data variable and their respective transformations. All data vintages were gathered from the St. Louis ALFRED database.

We undertake our real-time nowcasting application between January 2016 and March 2022, and we focus on generating the nowcasts and forecasts under three release timings of the US real GDP. Furthermore, we follow an expanding window approach where our initial training sample (or hold out) period is from January 1973 to December 2015. As our application is a real-time exercise, we respect the release calendar for monthly and quarterly variables; therefore, we face ragged edges at the end of the sample, mainly due to the release delay of real GDP relative to the monthly indicators.

| Description | Fred Mnemonic | Frequency | Transformation |
|---|---|---|---|
| Average Weekly Hours | AWHMAN | Monthly | $0.1 \times x_t$ |
| CPI Inflation | CPIAUCSL | Monthly | $100 \triangle \ln x_t$ |
| Industrial Production | INDPRO | Monthly | $100 \triangle \ln x_t$ |
| S&P 500 | S&P500 | Monthly | $100 \triangle \ln x_t$ |
| Federal Funds Rate | FEDFUNDS | Monthly | Level |
| 10 years Government Treasury yield | GS10 | Monthly | Level |
| Unemployment Rate | UNRATE | Monthly | Level |
| Chicago Fed National Financial Condition Index | NFCI | Monthly | Level |
| Real Gross Domestic Product | GDPC1 | Quarterly | $400 \triangle \ln x_t$ |

Table 1: Data information.

| Description | Ragged-edge at the end of sample | Nowcast Classification |
|---|---|---|
| US Real GDP has no release delay | No | Forecast |
| US Real GDP has a release delay of one month | Yes | Nowcast $T + 1$ |
| US Real GDP has a release delay of two months | Yes | Nowcast $T + 2$ |

Table 2: Classifications of Nowcasts.

Table 2 describes the three specific types of nowcasts that we produce from our model according to the release delay of the US real GDP. In particular, exploiting the proposed quantile regression framework, we focus on the growth-at-risk nowcasts based on the 10th percentile, $\tau = 0.1$. For completeness, we also generate the nowcasts for the 50th ($\tau = 0.5$) and 90th ($\tau = 0.9$) percentiles to further investigate the behavior of the entire distribution of real GDP. The first type of nowcast is a standard forecast since the US real GDP has no release delay relative to the monthly variables under this category. In this case, both the monthly and quarterly US GDP variables have a balanced data structure, and no ragged edge occurs at the end of the sample. Thus, a growth-at-risk forecast is made for one to three months ahead. The second and third types of nowcasts are produced from our model when the US real GDP is released with a one- and two-month delay, respectively. In both cases, the monthly and quarterly US GDP variables have an unbalanced data structure and a ragged edge at the end of the sample. Therefore, nowcasts of growth-at-risk are made under both categories.

Figure 1 plots the rolling three-month posterior mean average of the monthly changes of the growth-at-risk estimates for the three types of nowcasts. It is evident from Figure 1 that the growth-at-risk nowcasts were, on average, about -3% during the pre-pandemic period, whereas this average has fallen to about -5% since the pandemic. This implies that COVID-19 has caused US monthly real GDP to be more skewed to the left and increased the vulnerability of the US to enter a recession. In contrast, considering the 50th and 90th percentile, the monthly nowcast between spring and summer 2020 evolved in opposite direction compared to the quarterly predictions (see the Supplementary Material). This further highlights the importance of the proposed nowcasting approach in providing a timely characterization of risks.

Moreover, for comparison purposes, in Fig. 1 we also plot the corresponding quarterly growth-at-risk nowcasts from a U-MIDAS quantile regression (QR) model. This U-MIDAS QR model extends the quarterly frequency QR model used in Adrian et al. (2019) and includes a monthly NFCI instead of a quarterly series utilized by Adrian et al.
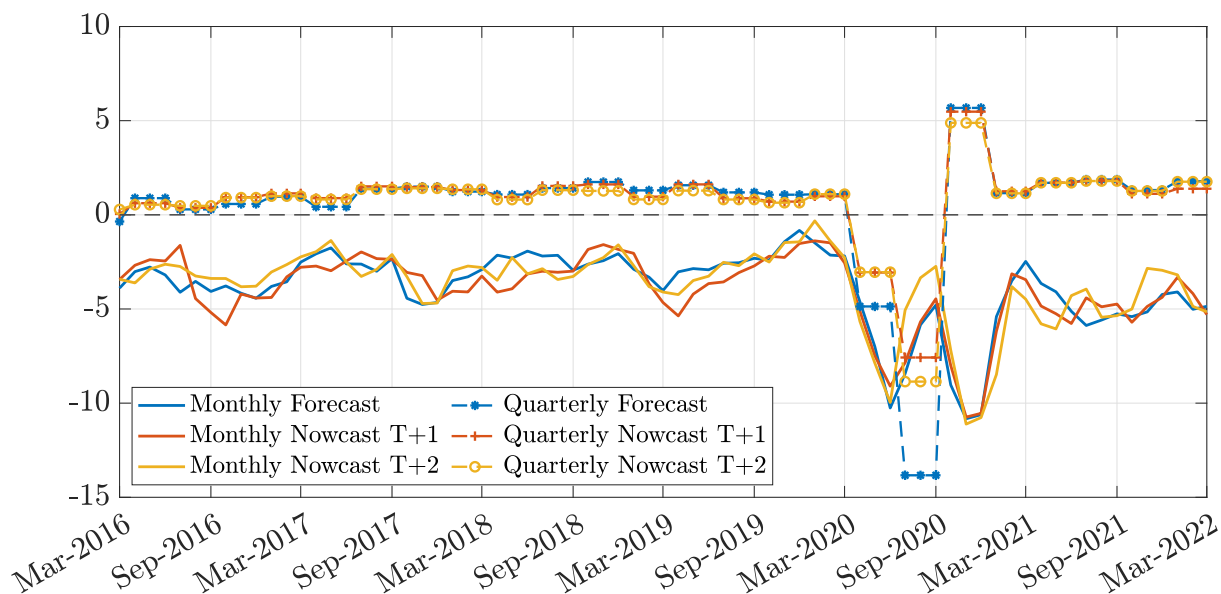
Figure 1: Posterior mean of the rolling three-month average growth-at-risk changes for the 10th percentile ($\tau = 0.1$), from MF-QVAR (monthly, solid), and U-MIDAS QR (quarterly, dashed). Forecasts of $T$ in blue, nowcasts of $T + 1$ in red, and nowcasts of $T + 2$ in yellow.

(2019). The resulting quarterly growth-at-risk nowcasts are denoted as the dashed lines in Fig. 1. Most of these quarterly growth-at-risk nowcasts are positive, except for the initial year of the COVID-19 pandemic. In contrast, the monthly growth-at-risk nowcasts from the MF-QVAR model are all negative. These results suggest that the nowcasts from the U-MIDAS QR model may be underestimating the underlying growth-at-risk measure for US Real GDP. For instance, the growth-at-risk nowcasts from the U-MIDAS QR model bounce back to their pre-pandemic level in 2021, which is inconsistent with recent global events. In fact, since the pandemic period, the US has experienced weaker growth and high inflation, and intuitively one would expect the US to be more prone to a recession than an expansion. Conversely, the nowcasting results from our MF-QVAR model are consistent with this idea.

To further investigate the skewness of the real GDP nowcasts, we also generated the nowcasts for the 50th ($\tau = 0.5$) and 90th ($\tau = 0.9$) percentiles. Figure 2 plots all the posterior estimates of the percentiles for the monthly nowcast of $T + 2$. The pattern displayed in Fig. 2 indeed confirms our previous finding that the COVID-19 pandemic has caused the real GDP nowcasts to become more negatively skewed. Similar

17

conclusions can be drawn from the monthly forecast and monthly nowcast of $T + 1$ (see the Supplementary Material). Moreover, in Table 3 we report the posterior monthly nowcasts of all the percentiles for selected pandemic periods. For December 2019, the nowcast estimate for the 10th percentile was -1.44%, dropping to -5.67% in April 2020 of the first wave of the pandemic. In addition, the uncertainty associated with the real GDP nowcasts appears to have widened since the pandemic. For example, in Table 3, the distance between the nowcasts of the 10th and 90th percentile has significantly increased since December 2019. This result suggests that nowcasting real GDP has become inherently challenging since the pandemic.
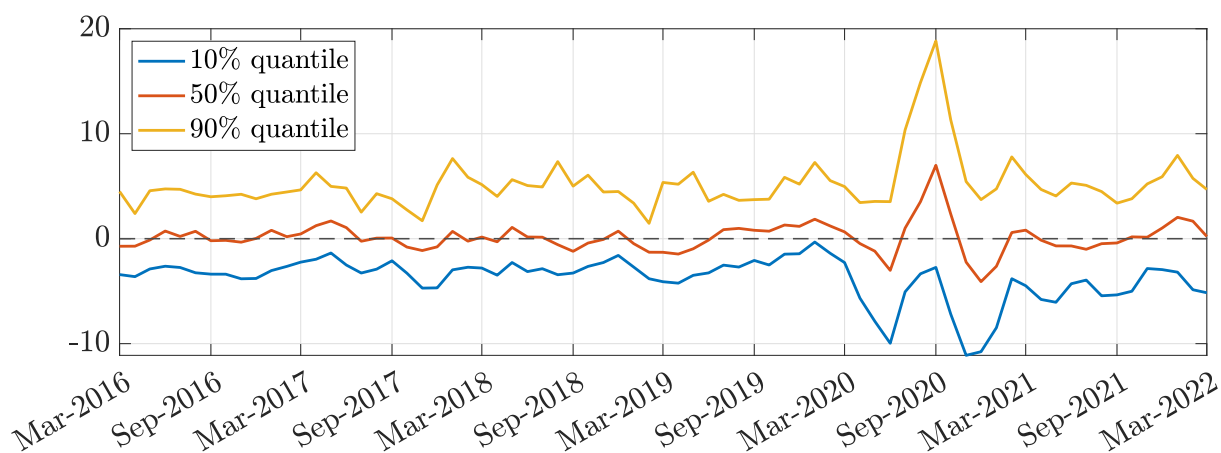


Figure 2: Posterior mean of the rolling three-month average of the Monthly Nowcast $T + 2$ for the 10th ($\tau = 0.1$, blue), 50th ($\tau = 0.5$, red), and 90th percentile ($\tau = 0.9$, yellow).

|  | Percentile | | | |
| Dates | $\tau = 0.1$ | $\tau = 0.5$ | $\tau = 0.9$ | Difference between $\tau = 0.9$ and $\tau = 0.1$ |
| --- | --- | --- | --- | --- |
| December 2019 | -1.44 | 1.17 | 5.20 | 6.63 |
| April 2020 | -5.67 | -0.46 | 3.44 | 9.11 |
| September 2020 | -2.74 | 6.99 | 18.84 | 21.58 |
| January 2021 | -8.48 | -2.63 | 4.75 | 13.23 |
| December 2021 | -2.95 | 1.01 | 5.90 | 8.85 |

Table 3: Posterior estimates of the 10th, 50th and 90th percentiles for the monthly nowcast $T + 1$ across selected periods during the pandemic period.

## 4.1 Does a tightening of the NFCI have a negative impact on US growth-at-risk?

In this section, we conduct a counterfactual analysis to investigate the importance of NFCI in a nowcasting monthly US growth-at-risk. Specifically, we undertake the same real-time out-of-sample forecasting exercise described in the preceding section. In addition, for each window of nowcast made, we assume a tightening of the NFCI in the last three months, holding all other things constant. This will allow us to explicitly determine whether a tightening of the NFCI does indeed negatively impact monthly nowcasts of US growth-at-risk.

Figure 3 plots the posterior mean differences of the counterfactual and the actual real-time nowcasts for the three cases with their associated 68% credible intervals. The posterior estimates were first calculated by taking the difference between each MCMC draw of the counterfactual and actual real-time nowcasts. Next, the average was computed across these differences. In general, a tightening of the NFCI appears to have a statistically significant negative impact on the monthly forecast and nowcast of $T + 2$. However, for the monthly nowcast $T + 1$, a tightening of the NFCI appears to have a

muted effect. Furthermore, Table 4 reports the averages of these differences over the evaluation period. A tightening of the NFCI appears to cause a deterioration in the monthly growth-at-risk forecast and nowcast of $T + 2$ by about 2-2.6% on average.

These results infer that NFCI significantly impacts forecasts and nowcasts of monthly US growth-at-risk. In particular, NFCI significantly influences the nowcasts of growth-at-risk on months when US real GDP has a release delay of two months. Therefore, our results reinforce the Adrian et al. (2019) findings and further highlight the importance of including NFCI in a mixed frequency setting when modeling growth-at-risk.

**(a) Monthly Forecast**



**(b) Monthly Nowcast $T + 1$**


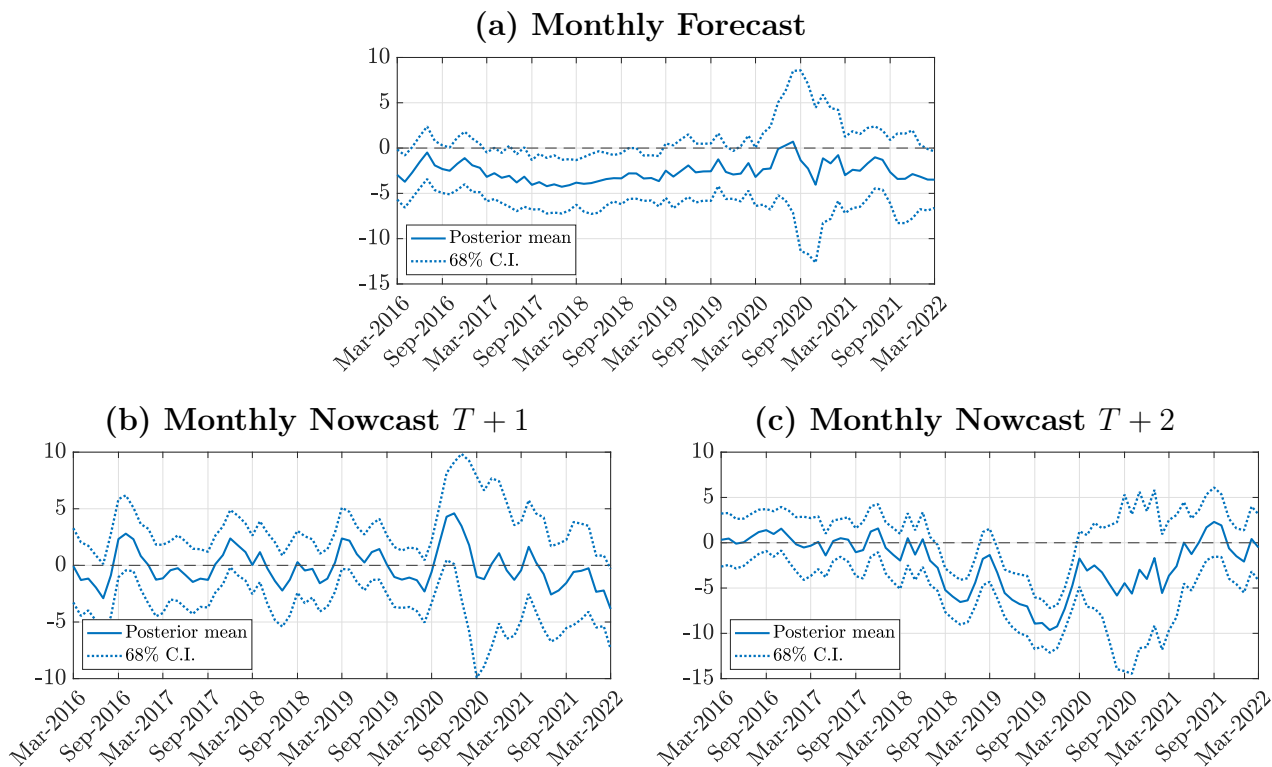
**(c) Monthly Nowcast $T + 2$**

Figure 3: Posterior mean differences of the counterfactual and the actual real-time nowcasts (thick line) and the associated 68% credible interval (dotted line), for time $T$, $T + 1$, and $T + 2$.

| Percentiles | Forecast | Nowcast $T+1$ | Nowcast $T+2$ |
|---|---|---|---|
| 10th Percentile | -2.63 | -0.13 | -2.23 |
| 50th Percentile | -1.82 | 0.31 | -0.68 |
| 90th Percentile | 1.35 | 1.32 | 2.04 |

Table 4: The average posterior mean differences of the counterfactual and the actual real-time nowcasts across the out-of-sample evaluation period.

# 5    Conclusions

Motivated by the limitations of popular VAR models for low-frequency economic variables, we introduce a novel mixed-frequency quantile vector autoregression (MF-QVAR) model. The proposed method exploits the informational content of high- and low-frequency variables to produce forecasts and nowcasts of conditional quantiles for indicators of interest. This permits to derive quantile-related risk measures at high frequency, thus enabling timely policy interventions.

The MF-QVAR model admits a state-space representation where the measurement follows a multivariate asymmetric Laplace distribution. Bayesian inference is performed by means of an efficient MCMC algorithm that exploits a data augmentation scheme coupled with a precision sampler to estimate the missing low-frequency variables at higher frequencies.

The proposed method is applied to US macroeconomic data to obtain real-time nowcasts for the growth-at-risk of US real GDP. The results show the ability of MF-QVAR to produce meaningful monthly nowcasts that outperform the quarterly U-MIDAS QR benchmark and reveal interesting patterns at the outbreak and during the COVID-19 pandemic. Moreover, a counterfactual analysis reveals that a contraction of NFCI has a negative and significant impact on the forecasts and nowcasts of monthly US growth-at-risk.

# References

Adams, P. A., T. Adrian, N. Boyarchenko, and D. Giannone (2021). Forecasting macroeconomic risks. *International Journal of Forecasting 37*(3), 1173–1191.

Adrian, T., N. Boyarchenko, and D. Giannone (2019). Vulnerable growth. *American Economic Review 109*(4), 1263–89.

Berger, T., J. Morley, and B. Wong (2020). Nowcasting the output gap. *Journal of Econometrics*.

Bernardi, M., G. Gayraud, and L. Petrella (2015). Bayesian tail risk interdependence using quantile regression. *Bayesian Analysis 10*(3), 553–603.

Bhadra, A., J. Datta, N. G. Polson, and B. Willard (2016). Default Bayesian analysis with global-local shrinkage priors. *Biometrika 103*(4), 955–969.

Caggiano, G., E. Castelnuovo, and G. Nodari (2022). Uncertainty and monetary policy in good and bad times: A replication of the vector autoregressive investigation by bloom (2009). *Journal of Applied Econometrics 37*(1), 210–217.

Casarin, R., C. Foroni, M. Marcellino, and F. Ravazzolo (2018). Uncertainty through the lenses of a mixed-frequency Bayesian panel Markov-switching model. *The Annals of Applied Statistics 12*(4), 2559–2586.

Chan, J. C. and I. Jeliazkov (2009). Efficient simulation and integrated likelihood estimation in state space models. *International Journal of Mathematical Modelling and Numerical Optimisation 1*(1-2), 101–120.

Chan, J. C., G. Koop, and S. M. Potter (2013). A new model of trend inflation. *Journal of Business & Economic Statistics 31*(1), 94–106.

Chan, J. C., A. Poon, and D. Zhu (2021). Efficient estimation of state-space mixed-frequency VARs: A precision-based approach. *arXiv preprint arXiv:2112.11315*.

Chavleishvili, S. and S. Manganelli (2021). Forecasting and Stress Testing with Quantile Vector Autoregression. Technical Report 2330, ECB Working Paper.

Cimadomo, J., D. Giannone, M. Lenza, F. Monti, and A. Sokol (2021). Nowcasting with large Bayesian vector autoregressions. *Journal of Econometrics*.

Cong, Y., B. Chen, and M. Zhou (2017). Fast simulation of hyperplane-truncated multivariate normal distributions. *Bayesian Analysis 12*(4), 1017–1037.

Durbin, J. and S. J. Koopman (2002). A simple and efficient simulation smoother for state space time series analysis. *Biometrika 89*(3), 603–616.

Durbin, J. and S. J. Koopman (2012). *Time series analysis by state space methods*, Volume 38. OUP Oxford.

Ghysels, E. (2016). Macroeconomics and the reality of mixed frequency data. *Journal of Econometrics 193*(2), 294–314.

Ghysels, E., P. Santa-Clara, and R. Valkanov (2005). There is a risk-return trade-off after all. *Journal of Financial Economics 76*(3), 509–548.

Ghysels, E., P. Santa-Clara, and R. Valkanov (2006). Predicting volatility: getting the most out of return data sampled at different frequencies. *Journal of Econometrics 131*(1-2), 59–95.

Gneiting, T. and R. Ranjan (2011). Comparing density forecasts using threshold- and quantile-weighted scoring rules. *Journal of Business & Economic Statistics 29*(3), 411–422.

Hauber, P. and C. Schumacher (2021). Precision-based sampling with missing observations: A factor model application. *Deutsche Bundesbank Discussion Paper*.

Huber, F., G. Koop, L. Onorante, M. Pfarrhofer, and J. Schreiner (2020). Nowcasting in a pandemic using non-parametric mixed frequency VARs. *Journal of Econometrics*.

Huber, F. and L. Rossini (2022). Inference in bayesian additive vector autoregressive tree models. *The Annals of Applied Statistics 16*(1), 104–123.

Hubrich, K. and R. J. Tetlow (2015). Financial stress and economic dynamics: The transmission of crises. *Journal of Monetary Economics 70*, 100–115.

Kadiyala, K. R. and S. Karlsson (1997). Numerical methods for estimation and inference in bayesian var-models. *Journal of Applied Econometrics 12*(2), 99–132.

Kaufmann, S. and C. Schumacher (2019). Bayesian estimation of sparse dynamic factor models with order-independent and ex-post mode identification. *Journal of Econometrics 210*(1), 116–134.

Khalaf, L., M. Kichian, C. J. Saunders, and M. Voia (2021). Dynamic panels with MIDAS covariates: Nonlinearity, estimation and fit. *Journal of Econometrics 220*(2), 589–605.

Kilian, L. and R. J. Vigfusson (2017). The role of oil price shocks in causing US recessions. *Journal of Money, Credit and Banking 49*(8), 1747–1776.

Koenker, R. and G. Bassett (1978). Regression quantiles. *Econometrica*, 33–50.

Koop, G., S. McIntyre, J. Mitchell, and A. Poon (2020). Regional output growth in the United Kingdom: More timely and higher frequency estimates from 1970. *Journal of Applied Econometrics 35*(2), 176–197.

Kotz, S., T. Kozubowski, and K. Podgórski (2001). *The Laplace distribution and generalizations: a revisit with applications to communications, economics, engineering, and finance.* Number 183. Springer Science & Business Media.

Mariano, R. S. and Y. Murasawa (2003). A new coincident index of business cycles based on monthly and quarterly series. *Journal of Applied Econometrics 18*(4), 427–443.

Mariano, R. S. and Y. Murasawa (2010). A coincident index, common factors, and monthly real GDP. *Oxford Bulletin of Economics and Statistics 72*(1), 27–46.

Merlo, L., L. Petrella, and V. Raponi (2021). Forecasting var and es using a joint quantile regression and its implications in portfolio allocation. *Journal of Banking & Finance 133*, 106248.

Mogliani, M. and A. Simoni (2021). Bayesian MIDAS penalized regressions: Estimation, selection, and prediction. *Journal of Econometrics 222*(1), 833–860.

Montes-Rojas, G. (2019). Multivariate Quantile Impulse Response Funcitons. *Journal of Time Series Analysis 40*, 739–752.

Neal, R. M. (2003, 6). Slice sampling. *The Annals of Statistics 31*(3), 705–767.

Petrella, L. and V. Raponi (2019). Joint estimation of conditional quantiles in multivariate linear regression models with an application to financial distress. *Journal of Multivariate Analysis 173*, 70–84.

Polson, N. G. and J. G. Scott (2010). Shrink globally, act locally: Sparse Bayesian regularization and prediction. *Bayesian Statistics 9*(501-538), 105.

Rue, H. (2001). Fast sampling of Gaussian Markov random fields. *Journal of the Royal Statistical Society: Series B (Statistical Methodology) 63*(2), 325–338.

Rue, H. and L. Held (2005). *Gaussian Markov random fields: Theory and applications.* Chapman and Hall/CRC.

Schorfheide, F. and D. Song (2015). Real-time forecasting with a mixed-frequency VAR. *Journal of Business & Economic Statistics 33*(3), 366–380.

Schorfheide, F., D. Song, and A. Yaron (2018). Identifying long-run risks: A Bayesian mixed-frequency approach. *Econometrica 86*(2), 617–654.

Tian, Y., E. Li, and M. Tian (2016). Bayesian joint quantile regression for mixed effects models with censoring and errors in covariates. *Computational Statistics 31*(3), 1031–1057.

Tian, Y.-Z., M.-L. Tang, and M.-Z. Tian (2021). Bayesian joint inference for multivariate quantile regression model with $L_{1/2}$ penalty. *Computational Statistics 36*(4), 2967–2994.

Tobias, A. and M. K. Brunnermeier (2016). CoVaR. *American Economic Review 106*(7), 1705.

Yu, K. and R. A. Moyeed (2001). Bayesian quantile regression. *Statistics & Probability Letters 54*(4), 437–447.

# A   Asymmetric Laplace distribution

**Univariate case.**   A random number $y \in \mathbb{R}$ follows an asymmetric Laplace distribution, denoted $y \sim \mathcal{AL}(\mu, \sigma, \tau)$, if

$$f(y|\mu, \sigma, \tau) = \frac{\tau(1-\tau)}{\sigma} \exp\left\{ -\rho\left(\frac{y-\mu}{\sigma}\right) \right\},$$

where $\rho(\cdot)$ denotes the check loss function, $\sigma > 0$, $\mu \in \mathbb{R}$ and $\tau \in (0,1)$ are the scale, location, and skewness parameters, respectively. The asymmetric Laplace distribution admits a representation as a location-scale mixture of Gaussian distributions, with exponentially-distributed mixing variable (Petrella and Raponi, 2019; Kotz et al., 2001), as follows:

$$y = \mu + w\sigma\theta_{\tau,1} + \sigma\theta_{\tau,2}\sqrt{w}z, \qquad z \sim \mathcal{N}(0,1) \quad w \sim \mathcal{E}xp(1),$$

where the rate parametrization of the exponential distribution is used[2] and

$$\theta_{\tau,1} = \frac{1-2\tau}{\tau(1-\tau)}, \qquad \theta_{\tau,2} = \sqrt{\frac{2}{\tau(1-\tau)}}.$$

Therefore, it holds:

$$f(y|\mu,\sigma,\tau) = \int_0^{+\infty} \exp\{-w\}\left(2\pi\sigma^2\theta_{\tau,2}^2 w\right)^{-\frac{1}{2}} \exp\left\{-\frac{(y-\mu-\sigma\theta_{\tau,1}w)}{2\sigma^2\theta_{\tau,2}^2 w}\right\} \, dw.$$

**Multivariate case.** An $n$-dimensional random vector $\mathbf{y} \in \mathbb{R}^n$ follows a multivariate asymmetric Laplace distribution, denoted $\mathbf{y} \sim \text{MAL}_n(\boldsymbol{\mu}, D\boldsymbol{\theta}_{\tau,1}, D\boldsymbol{\theta}_{\tau,2}\Psi\boldsymbol{\theta}_{\tau,2}D)$, if

$$\mathbf{y} = \boldsymbol{\mu} + wD\boldsymbol{\theta}_{\tau,1} + \sqrt{w}D\boldsymbol{\theta}_{\tau,2}^{1/2}\Psi^{1/2}\mathbf{z}, \qquad w \sim \mathcal{E}xp(1), \quad \mathbf{z} \sim \mathcal{N}_n(0, I_n),$$

where $\Psi$ is a correlation matrix, $D = \text{diag}(\delta_1, \ldots, \delta_n)$, and

$$\boldsymbol{\theta}_{\tau,1} = \left(\frac{1-2\tau_1}{\tau_1(1-\tau_1)}, \ldots, \frac{1-2\tau_n}{\tau_n(1-\tau_n)}\right)', \qquad \boldsymbol{\theta}_{\tau,2} = \text{diag}\left(\sqrt{\frac{2}{\tau_1(1-\tau_1)}}, \ldots, \sqrt{\frac{2}{\tau_n(1-\tau_n)}}\right).$$

This implies that each entry $y_i$ is given by

$$y_i = \mu_i + w\delta_i\theta_{\tau,1,i} + \sqrt{w}\delta_i\theta_{\tau,2,i}z_i, \qquad w \sim \mathcal{E}xp(1), \quad z_i \sim \mathcal{N}(0, 1),$$

thus providing

$$y_i \sim \mathcal{AL}(\mu_i, \delta_i, \tau_i).$$

---

[2]Using the rate parametrization of the exponential distribution, it holds $k\mathcal{E}xp(\sigma) \overset{d}{=} \mathcal{E}xp(\sigma/k)$.